J|A|C|S

ARTICLES

Published on Web 11/20/2003

A Molecular Switch in Amyloid Assembly: Met^{35} and Amyloid β-Protein Oligomerization

Gal Bitan,[†] Bogdan Tarus,[‡] Sabrina S. Vollers,[†] Hilal A. Lashuel,[†] Margaret M. Condron,[†] John E. Straub,[‡] and David B. Teplow*,[†]

Contribution from the Center for Neurologic Diseases, Brigham and Women's Hospital, and Department of Neurology, Harvard Medical School, Boston, Massachusetts 02115, and Department of Chemistry, Boston University, Boston, Massachusetts 02215

Received February 28, 2003; E-mail: teplow@cnd.bwh.harvard.edu.

Abstract: Aberrant protein oligomerization is an important pathogenetic process in vivo. In Alzheimer's disease (AD), the amyloid β-protein (Aβ) forms neurotoxic oligomers. The predominant in vivo Aβ alloforms, Aβ40 and Aβ42, have distinct oligomerization pathways. Aβ42 monomers oligomerize into pentamer/hexamer units (paranuclei) which self-associate to form larger oligomers. Aβ40 does not form these paranuclei, a fact which may explain the particularly strong linkage of Aβ42 with AD. Here, we sought to determine the structural elements controlling paranucleus formation as a first step toward the development of strategies for treating AD. Because oxidation of Met^{35} is associated with altered Aβ assembly, we examined the role of Met^{35} in controlling Aβ oligomerization. Oxidation of Met^{35} in Aβ42 blocked paranucleus formation and produced oligomers indistinguishable in size and morphology from those produced by Aβ40. Systematic structural alterations of the $C_{\gamma}{}^{35}$-substituent group revealed that its electronic nature, rather than its size (van der Waals volume), was the factor controlling oligomerization pathway choice. Preventing assembly of toxic Aβ42 paranuclei through selective oxidation of Met^{35} thus represents a potential therapeutic approach for AD.

Introduction

Amyloid β-protein (Aβ) is the main proteinaceous component of the amyloid plaques found in the brains of Alzheimer's disease (AD) patients.[1,2] Neuritic plaques, pathognomonic features of AD, contain abundant fibrils formed from Aβ. These fibrils have been found to be neurotoxic in vivo and in vitro.[3−5] Recent studies of structure−activity relationships among fibril assembly intermediates have revealed that many intermediates are neurotoxic, including dimers and trimers,[6] Aβ-derived diffusible ligands (ADDLs),[7] and protofibrils.[8,9] These oligomers may, in fact, be the proximal effectors of neuropathogenesis in AD.[10−12] This new insight into the assembly and biological activity of fibril precursors suggests that therapeutic strategies may need to target oligomeric assemblies. To facilitate the development of these strategies, an understanding of the mechanisms controlling the formation of oligomeric Aβ assemblies is necessary.

The predominant forms of Aβ found in brains of AD patients are 40 and 42 amino acids long (designated Aβ40 and Aβ42, respectively).[13,14] Despite the small primary structure difference between Aβ40 and Aβ42, i.e., the dipeptide Ile^{41}-Ala^{42}, the clinical impact and biophysical behavior of the two Aβ alloforms are distinct. Aβ40 and Aβ42 exist in the plasma and cerebrospinal fluid at a concentration ratio of ~10:1, respectively, yet Aβ42 is deposited first during the development of AD [15,16] and is more neurotoxic than Aβ40.[17,18] Alloform-specific patterns of amyloid deposition are observed. Aβ42 is the predominant

[†] Center for Neurologic Diseases, Brigham and Women's Hospital, and Department of Neurology, Harvard Medical School.

[‡] Department of Chemistry, Boston University.

(1) Glenner, G. G.; Wong, C. W. *Biochem. Biophys. Res. Commun.* **1984**, *120*, 885−890.
(2) Masters, C. L.; Simms, G.; Weinman, N. A.; Multhaup, G.; McDonald, B. L.; Beyreuther, K. *Proc. Natl. Acad. Sci. U.S.A.* **1985**, *82*, 4245−4249.
(3) Pike, C. J.; Walencewicz, A. J.; Glabe, C. G.; Cotman, C. W. *Brain Res.* **1991**, *563*, 311−314.
(4) Lorenzo, A.; Yankner, B. A. *Proc. Natl. Acad. Sci. U.S.A.* **1994**, *91*, 12 243−12 247.
(5) Geula, C.; Wu, C. K.; Saroff, D.; Lorenzo, A.; Yuan, M. L.; Yankner, B. A. *Nature Med.* **1998**, *4*, 827−831.
(6) Walsh, D. M.; Klyubin, I.; Fadeeva, J. V.; Cullen, W. K.; Anwyl, R.; Wolfe, M. S.; Rowan, M. J.; Selkoe, D. J. *Nature* **2002**, *416*, 535−539.
(7) Lambert, M. P.; Barlow, A. K.; Chromy, B. A.; Edwards, C.; Freed, R.; Liosatos, M.; Morgan, T. E.; Rozovsky, I.; Trommer, B.; Viola, K. L.; Wals, P.; Zhang, C.; Finch, C. E.; Krafft, G. A.; Klein, W. L. *Proc. Natl. Acad. Sci. U.S.A.* **1998**, *95*, 6448−6453.
(8) Walsh, D. M.; Hartley, D. M.; Kusumoto, Y.; Fezoui, Y.; Condron, M. M.; Lomakin, A.; Benedek, G. B.; Selkoe, D. J.; Teplow, D. B. *J. Biol. Chem.* **1999**, *274*, 25 945−25 952.
(9) Hartley, D. M.; Walsh, D. M.; Ye, C. P. P.; Diehl, T.; Vasquez, S.; Vassilev, P. M.; Teplow, D. B.; Selkoe, D. J. *J. Neurosci.* **1999**, *19*, 8876−8884.
(10) Klein, W. L.; Krafft, G. A.; Finch, C. E. *Trends Neurosci.* **2001**, *24*, 219−224.
(11) Kirkitadze, M. D.; Bitan, G.; Teplow, D. B. *J. Neurosci. Res.* **2002**, *69*, 567−577.
(12) Walsh, D. M.; Klyubin, I.; Fadeeva, J. V.; Rowan, M. J.; Selkoe, D. J. *Biochem. Soc. Trans.* **2002**, *30*, 552−557.
(13) Selkoe, D. J. *Physiol. Rev.* **2001**, *81*, 741−766.
(14) Gravina, S. A.; Ho, L. B.; Eckman, C. B.; Long, K. E.; Otvos, L., Jr.; Younkin, L. H.; Suzuki, N.; Younkin, S. G. *J. Biol. Chem.* **1995**, *270*, 7013−7016.
(15) Suzuki, N.; Cheung, T. T.; Cai, X.-D.; Odaka, A.; Otvos, L., Jr; Eckman, C.; Golde, T. E.; Younkin, S. G. *Science* **1994**, *264*, 1336−1340.
(16) Gravina, S. A.; Ho, L. B.; Eckman, C. B.; Long, K. E.; Otvos, L., Jr; Younkin, L. H.; Suzuki, N.; Younkin, S. G. *J. Biol. Chem.* **1995**, *270*, 7013−7016.
(17) Younkin, S. G. *Ann. Neurol.* **1995**, *37*, 287−288.
(18) Dahlgren, K. N.; Manelli, A. M.; Stine, W. B., Jr.; Baker, L. K.; Krafft, G. A.; LaDu, M. J. *J. Biol. Chem.* **2002**, *277*, 32 046−32 053.

component in parenchymal plaques, whereas Aβ40 is the predominant component in vascular deposits.[19,20] An increase in the Aβ42/Aβ40 ratio is associated with early onset familial AD.[21,22] Oligomeric Aβ42 has been shown to be toxic to neuronal cells at nanomolar levels in vitro,[7,23−29] whereas Aβ40 oligomers are significantly less toxic.[18,30] In addition, Aβ42 has been shown to form fibrils substantially faster than Aβ40.[31,32]

Recently, we demonstrated that the early assembly of Aβ42 involves formation of pentamer/hexamer units termed paranuclei.[33] Following their formation, paranuclei self-associate into larger oligomers, which appear to give rise to protofibrils.[33] Paranucleus formation is the earliest observable Aβ42 assembly event. Early Aβ40 assembly produces an equilibrium mixture of monomer, dimer, trimer, and tetramer.[34] Assemblies in this mixture are largely amorphous, in contrast to the quasiglobular paranuclei observed in Aβ42 preparations.[33] These biophysical differences between Aβ40 and Aβ42 are likely to underlie the distinct biological behaviors of the two peptides. Therapeutic agents capable of directing Aβ42 down oligomerization pathways akin to that of Aβ40, i.e., delaying or inhibiting paranucleus formation and self-association, thus could be of clinical value.

It has been postulated that Met^{35} contributes to the neurotoxic activity of Aβ. In particular, oxidation of Met^{35} to the corresponding sulfoxide (Met(O)^{35}) has been suggested to be involved in Aβ-induced oxidative damage.[35,36] However, a confusing observation is that the toxicity of Aβ increases with assembly of the monomeric peptide into oligomers and fibrils, but its oxidative power is highest for monomers and decreases with assembly.[37] In addition, solution NMR studies of reduced and oxidized Aβ40 and Aβ42 have shown little conformational difference among the four peptides,[38] suggesting that the effect of Met^{35} on the biological activity of Aβ is exerted in the assembled state, rather than in the monomeric state. [Met(O)^{35}]Aβ has been reported to display both accelerated[39,40] and delayed[41] fibrillogenesis rates relative to wild type (WT) Aβ. The biological implications of these data are unclear. Recent reports have shown that formation of small oligomers by Aβ40[42] and of protofibrils by Aβ40[43] and Aβ42[44] is delayed upon Met^{35} oxidation. If oligomeric assemblies, rather than fibrils, are the key effectors of neurotoxicity in AD, then differences in assembly kinetics may not underlie the differences in biological activity between the reduced (native) and oxidized Aβ forms. Rather, the distinct neurotoxic activity of different Aβ alloforms may reflect qualitative differences such as formation or stabilization of particular oligomeric assemblies. Here, we examined the effect of Met^{35} oxidation on the oligomer size distribution of Aβ40 and Aβ42 using the technique of Photoinduced Cross-linking of Unmodified Proteins (PICUP).[45,46] PICUP provides the means to identify and quantitate small, metastable oligomers. These analyses are difficult using other biochemical or biophysical methods.[34] The current study reveals that oxidation of Met^{35} transforms the oligomer size distribution of Aβ42 into one that is indistinguishable from that of Aβ40, suggesting a key role for Met^{35} in the formation of paranuclei and in the control of oligomerization pathway choice.

Results

Characterization of the Oligomer Size Distributions of Reduced and Oxidized Aβ40 and Aβ42. To determine the effects of oxidation of Met^{35} to Met-sulfoxide [Met(O)^{35}] on the oligomer size distributions of Aβ40 and Aβ42, low molecular weight (LMW[47]) fractions of the reduced and oxidized peptides were isolated using size exclusion chromatography (SEC) and immediately cross-linked. SDS-PAGE analysis of cross-linked wild-type (WT) and oxidized Aβ40 revealed little difference between the oligomer size distributions (Figure 1A, lanes 1 and 3). Both distributions showed comparable abundances of monomer through tetramer, followed by a sharp decrease of the abundances of pentamer through heptamer, as described previously.[34] The distribution of WT Aβ42 comprised three groups of oligomers (Figure 1A, lane 2): monomer through trimer, displaying decreasing intensity with increasing oligomer order; a Gaussian-like distribution between tetramer and octamer, with a maximum at pentamer and hexamer; and oligomers of $M_r \approx 30-60$ kDa showing intensity maxima consistent with dodecamer and octadecamer. In contrast, the oligomer size distribution of [Met(O)^{35}]Aβ42 differed dramatically from that of WT Aβ42. It was, in fact, indistinguishable

(19) Suo, Z. M.; Humphrey, J.; Kundtz, A.; Sethi, F.; Placzek, A.; Crawford, F.; Mullan, M. *Neurosci. Lett.* **1998**, *257*, 77−80.
(20) Pillot, T.; Drouet, B.; Queille, S.; Labeur, C.; Vandekerckhove, J.; Rosseneu, M.; Pincon-Raymond, M.; Chambaz, J. *J. Neurochem.* **1999**, *73*, 1626−1634.
(21) Scheuner, D.; Eckman, C.; Jensen, M.; Song, X.; Citron, M.; Suzuki, N.; Bird, T. D.; Hardy, J.; Hutton, M.; Kukull, W.; Larson, E.; Levy-Lahad, E.; Viitanen, M.; Peskind, E.; Poorkaj, P.; Schellenberg, G.; Tanzi, R.; Wasco, W.; Lannfelt, L.; Selkoe, D. J.; Younkin, S. *Nature Med.* **1996**, *2*, 864−870.
(22) Golde, T. E.; Eckman, C. B.; Younkin, S. G. *Biochim. Biophys. Acta-Mol. Basis Dis.* **2000**, *1502*, 172−187.
(23) El-Agnaf, O. M.; Mahil, D. S.; Patel, B. P.; Austen, B. M. *Biochem. Biophys. Res. Commun.* **2000**, *273*, 1003−1007.
(24) Dahlgren, K. N.; Manelli, A. M.; Stine, W. B., Jr.; Baker, L. K.; Krafft, G. A.; LaDu, M. J. *J. Biol. Chem.* **2002**, *277*, 32 046−32 053.
(25) Wang, H. W.; Pasternak, J. F.; Kuo, H.; Ristic, H.; Lambert, M. P.; Chromy, B.; Viola, K. L.; Klein, W. L.; Stine, W. B.; Krafft, G. A.; Trommer, B. L. *Brain Res.* **2002**, *924*, 133−140.
(26) Gong, Y. S.; Chang, L.; Lambert, M. P.; Viola, K. L.; Krafft, G. A.; Finch, C. E.; Klein, W. L. *Soc. Neurosci. Abstr.* **2001**, *27*, 322.310.
(27) Tong, L. Q.; Thornton, P. L.; Balazs, R.; Cotman, C. W. *J. Biol. Chem.* **2001**, *276*, 17 301−17 306.
(28) Paris, D.; Town, T.; Mori, T.; Parker, T. A.; Humphrey, J.; Mullan, M. *Neurobiol. Aging* **2000**, *21*, 183−197.
(29) Hu, J. G.; Akama, K. T.; Krafft, G. A.; Chromy, B. A.; Van Eldik, L. J. *Brain Res.* **1998**, *785*, 195−206.
(30) Hoshi, M.; Sato, M.; Matsumoto, S.; Noguchi, A.; Yasutake, K.; Yoshida, N.; Sato, K. *Proc. Natl. Acad. Sci. U.S.A.* **2003**, *100*, 6370−6375.
(31) Jarrett, J. T.; Berger, E. P.; Lansbury, P. T., Jr. *Biochemistry* **1993**, *32*, 4693−4697.
(32) Jarrett, J. T.; Berger, E. P.; Lansbury, P. T., Jr. *Ann. N. Y. Acad. Sci.* **1993**, 144−148.
(33) Bitan, G.; Kirkitadze, M. D.; Lomakin, A.; Vollers, S. S.; Benedek, G. B.; Teplow, D. B. *Proc. Natl. Acad. Sci. U.S.A.* **2003**, *100*, 330−335.
(34) Bitan, G.; Lomakin, A.; Teplow, D. B. *J. Biol. Chem.* **2001**, *276*, 35 176−35 184.
(35) Butterfield, D. A.; Kanski, J. *Peptides* **2002**, *23*, 1299−1309.
(36) Schoneich, C. *Arch. Biochem. Biophys.* **2002**, *397*, 370−376.
(37) Varadarajan, S.; Kanski, J.; Aksenova, M.; Lauderback, C.; Butterfield, D. A. *J. Am. Chem. Soc.* **2001**, *123*, 5625−5631.
(38) Riek, R.; Guntert, P.; Döbeli, H.; Wipf, B.; Wuthrich, K. *Eur. J. Biochem.* **2001**, *268*, 5930−5936.
(39) Seilheimer, B.; Bohrmann, B.; Bondolfi, L.; Muller, F.; Stuber, D.; Döbeli, H. *J. Struct. Biol.* **1997**, *119*, 59−71.
(40) Snyder, S. W.; Ladror, U. S.; Wade, W. S.; Wang, G. T.; Barrett, L. W.; Matayoshi, E. D.; Huffaker, H. J.; Krafft, G. A.; Holzman, T. F. *Biophys. J.* **1994**, *67*, 1216−1228.
(41) Watson, A. A.; Fairlie, D. P.; Craik, D. J. *Biochemistry* **1998**, *37*, 12 700−12 706.
(42) Palmblad, M.; Westlind-Danielsson, A.; Bergquist, J. *J. Biol. Chem.* **2002**, *277*, 19 506−19 510.
(43) Johansson, A.-S.; Päiviö, A.; Lannfelt, L.; Westlind-Danielsson, A. *Neurobiol. Aging* **2002**, *23*, S187.
(44) Hou, L.; Kang, I.; Marchant, R. E.; Zagorski, M. G. *J. Biol. Chem.* **2002**, *277*, 40 173−40 176.
(45) Fancy, D. A.; Kodadek, T. *Proc. Natl. Acad. Sci. U.S.A.* **1999**, *96*, 6020−6024.
(46) Fancy, D. A.; Denison, C.; Kim, K.; Xie, Y. Q.; Holdeman, T.; Amini, F.; Kodadek, T. *Chem. Biol.* **2000**, *7*, 697−708.
(47) Walsh, D. M.; Lomakin, A.; Benedek, G. B.; Condron, M. M.; Teplow, D. B. *J. Biol. Chem.* **1997**, *272*, 22 364−22 372.

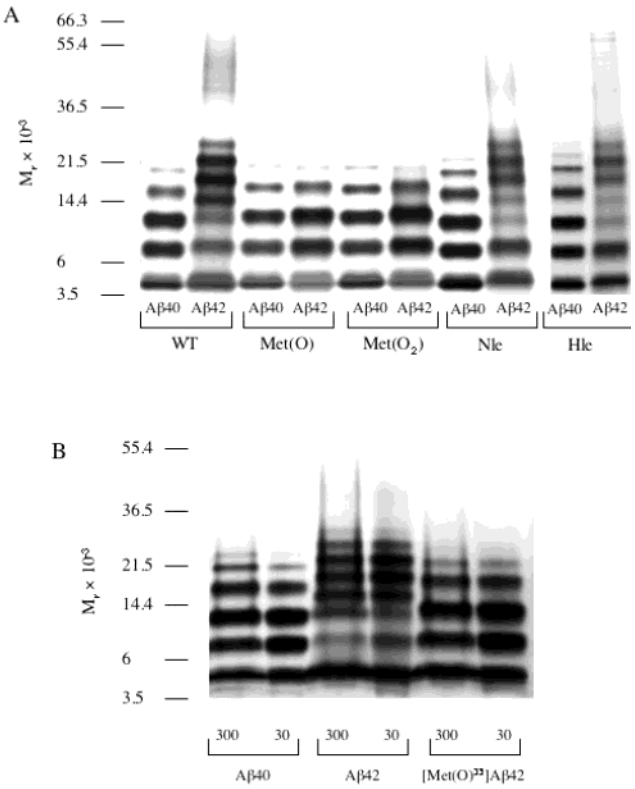

Figure 1. Effects of residue 35 side-chain structure and peptide concentration on **A**β oligomerization. A) PICUP was performed on SEC-isolated LMW Aβ40 and Aβ42 analogues containing the modifications $Met^{35} \rightarrow$ Met(O), $Met^{35} \rightarrow$ Met(O_2), $Met^{35} \rightarrow$ Nle, and $Met^{35} \rightarrow$ Hle. WT Aβ40 and Aβ42 were used as controls. Following cross-linking, the products were analyzed by SDS-PAGE and silver staining. Positions of molecular weight markers are shown on the left. The gel is representative of each of 3 independent experiments. B) PICUP was applied to freshly dissolved Aβ40, Aβ42, and $[Met(O)^{35}]$Aβ42 at nominal concentrations of 30 and 300 μM. Each peptide first was dissolved in water at a nominal concentration of 4 mg/mL. The pH then was adjusted to 10 by addition of 1N NaOH, after which 20 mM sodium phosphate, pH 7.4, was added to yield a final nominal peptide concentration of 300 μM. The solutions were sonicated for 1 min. Aliquots from these solutions were diluted 10-fold in 10 mM sodium phosphate, pH 7.4, to produce the 30 μM solutions. Following cross-linking, the products were analyzed by SDS-PAGE and silver staining. The volumes loaded were adjusted so that equal amounts of protein were loaded in each lane. Positions of molecular weight markers are shown on the left. The gel is representative of each of 3 independent experiments.

from the oligomer distributions of reduced and oxidized Aβ40 (Figure 1A, lane 4). This result suggested a crucial role for Met^{35} in the oligomerization of Aβ42, particularly in the formation of Aβ42 paranuclei. Moreover, the data demonstrated that the particular interactions leading to the oligomer size distribution observed for WT Aβ42, which of necessity involve Ile^{41} and $Ala^{42,33,48}$ were abolished by oxidation of Met^{35} to the corresponding sulfoxide.

In principle, the differences in the oligomerization patterns among Aβ42 and oxidized Aβ42 or Aβ40 may reflect solubility differences rather than distinct oligomerization behavior. If so, $[Met(O)^{35}]$Aβ42 and Aβ40, at higher concentrations, might form paranuclei. To address this question, we compared the oligomer size distributions of Aβ40, Aβ42, and $[Met(O)^{35}]$Aβ42 at nominal concentrations of 30 and 300 μM (Figure 1B). For all three alloforms, the oligomer size distributions obtained at 30 and 300 μM were essentially identical, demonstrating that the effect of oxidation on the oligomerization pattern was concentration-independent over this range of concentration, at a minimum.

Table 1. Calculated Dipole Moments and van der Waals Volumes for $C_\gamma{}^{35}$-Substituent

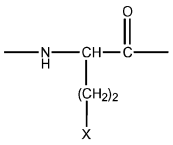

Residue	X	Dipole Moment (Debye)[a]	van der Waals volume (Å^3)[a]
Met	H_3C-S-	1.60	86.86
Met(O)	$H_3C-\overset{O}{\overset{\|}{S}}-$	5.28	96.35
Met(O_2)	$H_3C-\overset{O}{\overset{\|}{\underset{O}{\overset{\|}{S}}}}-$	5.20	102.70
Nle	H_3C-CH_2-	0.53	87.27
Hle	$H_3C-CH(CH_3)-$	0.58	106.65

[a] Values calculated for the chemical group X attached to the γ-methylene of residue 35.

Elucidation of Structural Elements at $C_\gamma{}^{35}$ which Control Aβ42 Paranucleus Formation. To determine the structural elements of residue 35 which affect paranucleus formation, three additional modifications were examined, oxidation of Met^{35} to Met-sulfone $[Met(O_2)^{35}]$ and substitutions by norleucine (Nle) and homoleucine (Hle). To compare the relative influence of electrostatic and steric forces, the dipole moments and van der Waals volumes of side chain portions beyond the γ-methylene were computed for each of the residues used (Table 1). Oxidation of Met to Met(O_2) is similar to oxidation to Met(O) in that it increases both the size and the polarity of the side chain (Table 1). Substitution of Met by Nle maintains the size and decreases the polarity of the side chain, whereas substitution by Hle increases the size and decreases the polarity (Table 1).

SEC-isolated LMW Aβ42 containing Met(O_2), Nle, or Hle in position 35 were cross-linked and analyzed by SDS-PAGE. The Aβ40 counterparts of these peptides were used as controls. The effect of oxidation of Met to Met(O_2) was identical to that of oxidation to Met(O) (cf., Figure 1A, lane 4 with lane 6). In fact, $[Met(O_2)^{35}]$Aβ42 yielded a distribution indistinguishable from those of $[Met(O)^{35}]$Aβ42 and all of the Aβ40 analogues examined (Figure 1A). By contrast, the distributions of $[Nle^{35}]$Aβ42 and $[Hle^{35}]$Aβ42 were qualitatively similar to that of WT Aβ42 (cf., Figure 1A, lanes 2, 8, and 10). They contained the same three groups of oligomers and the predominant cross-linking products were pentamer/hexamer. The relative abundance of the third oligomer group ($\sim$30$-$60 kDa) was decreased in the distributions of the Nle and Hle analogues, relative to WT Aβ42. The sulfur atom in residue 35 thus was not required for the formation of paranuclei, but the Met side chain facilitated the self-association of paranuclei more than the all-hydrocarbon side chains. The data suggest that the unique oligomer size

(48) Bitan, G.; Vollers, S. S.; Teplow, D. B. *J. Biol. Chem.* **2003**, *278*, 34 882−34 889.

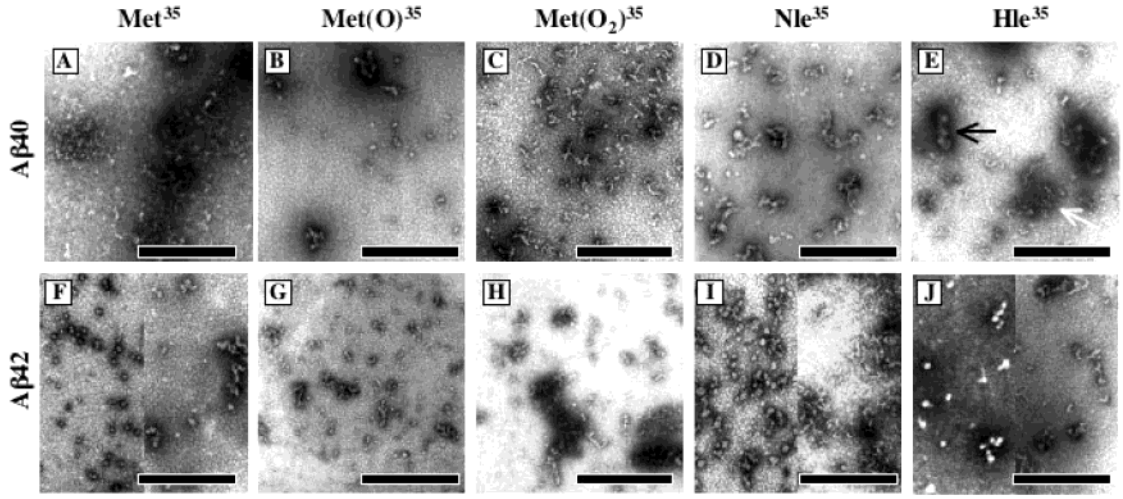

Figure 2. Morphologic analysis of LMW Aβ. Aβ40 (Panels A−E) and Aβ42 (panels F−J) containing Met^{35} (A,F), $Met(O)^{35}$ (B,G), $Met(O_2)^{35}$ (C,H), Nle^{35} (D,I), or Hle^{35} (E,J) were spotted on glow-discharged, carbon-coated grids immediately after isolation by SEC. The samples then were fixed with glutaraldehyde, stained with uranyl acetate, and examined by EM. Scale bars are 100 nm. The micrographs shown are representative of multiple fields recorded for each of several grids prepared in at least three independent experiments.

distribution of Aβ42 requires the hydrophobic, rather than the steric characteristics of Met^{35}. Thus, although the van der Waals volume of the Hle side chain is larger that those of Met(O) or $Met(O_2)$ (Table 1), the oligomer distribution of $[Hle^{35}]$Aβ42 was qualitatively similar to that of the WT peptide. The change in polarity, rather than the change in size, of the Met side chain thus appears responsible for the major alteration of the Aβ42 oligomer size distribution following oxidation. The oxidation of Met^{35} may destabilize paranuclei due to the increased energetic cost of desolvating the oxidized side chain (see Discussion).

Morphology of Aβ Oligomers. WT LMW Aβ40 and Aβ42 display distinct morphologies immediately following their preparation.[33] LMW Aβ40 is relatively amorphous whereas LMW Aβ42 produces quasi-globular structures ~2−10 nm in diameter. We determined here the effect of structural modifications at position 35 on the morphology of LMW Aβ (Figure 2). To do so, LMW fractions of each of the peptides used in the PICUP experiments were isolated and examined by EM. The morphology of oxidized Aβ42 resembled that of Aβ40.[33] The globular structures observed for WT Aβ42 were not detected for $[Met(O)^{35}]$Aβ42 or $[Met(O_2)^{35}]$Aβ42. The change in the morphology of oxidized Aβ42 relative to WT Aβ42 correlates with the distinct oligomer size distributions observed for the two peptides.

All Aβ40 analogues produced irregular, prolate aggregates. Two main classes were observed, one with mean diameter ~1−2 nm (Figure 2E white arrow) and the other with mean diameter ~5−10 nm (Figure 2E black arrow). WT and oxidized Aβ40 produced mainly the thinner structure whereas $[Nle^{35}]$Aβ40 and $[Hle^{35}]$Aβ40 produced more of the thicker structures. Similar structures also were observed for the Aβ42 analogues. However, WT Aβ42, $[Nle^{35}]$Aβ42, and $[Hle^{35}]$Aβ42 also showed quasi-spherical structures of diameter ~5−8 nm, either alone or associated into small groups. In agreement with the PICUP data, these quasi-spherical structures were not observed for $[Met(O)^{35}]$Aβ42 and $[Met(O_2)^{35}]$Aβ42, or for any of the Aβ40 analogues, supporting the conclusion that these morphologies correspond to paranuclei.[33]

Conformation of LMW Aβ40 and Aβ42 Analogues. We have shown previously that, immediately following isolation, LMW Aβ40 and Aβ42 both are predominantly unstructured.[33] To assess the conformational effects of side-chain modifications in position 35, the conformations of all the analogues used in this study were examined by CD immediately following their isolation by SEC (The CD spectra are available as Supporting Information). The predominant secondary structure element for all alloforms was "random coil." Small amounts of β-sheet, β-turn, and α-helix also were observed. The relative amounts of each structural element were similar for each of the analogues. These data show, as observed for WT Aβ, that the initial oligomerization of the analogues containing modifications in position 35 does not involve substantial conformational rearrangement.

Discussion

An important and contentious area in studies of the chemical biology of Alzheimer's disease is the role of redox chemistry and the involvement of Aβ in it. It has been suggested that the redox state of Met^{35} is critical in determining the biological activity of Aβ, yet the mechanism by which this effect is exerted is not well understood. One hypothesis proposes that oxidation of Met^{35}, possibly through interaction with transition metal ions, is directly related to generation of cytotoxic reactive oxygen species.[35,36] Alternatively, oxidative stress may be cellular in origin and result from the interaction of Aβ with neurons, microglia, and/or astrocytes.[49,50] If so, the assembly state of Aβ could be vital in controlling these cellular interactions. Consistent with this notion, Met^{35} oxidation has been reported to affect Aβ assembly. However, a consensus on precisely how Met^{35} does so does not exist. For example, it has been suggested that $[Met(O)^{35}]$Aβ forms fibrils faster,[39,40] at a similar rate,[37,51] or slower[38,41] than does WT Aβ. Recent studies have reported

(49) Perry, G.; Nunomura, A.; Hirai, K.; Zhu, X. W.; Perez, M.; Avila, J.; Castellani, R. J.; Atwood, C. S.; Aliev, G.; Sayre, L. M.; Takeda, A.; Smith, M. A. *Free Rad. Biol. Med.* **2002**, *33*, 1475−1479.
(50) Pratico, D. *Biochem. Pharmacol.* **2002**, *63*, 563−567.
(51) Döbeli, H.; Draeger, N.; Huber, G.; Jakob, P.; Schmidt, D.; Seilheimer, B.; Stuber, D.; Wipf, B.; Zulauf, M. *Bio/Technology* **1995**, *13*, 988−993.

that oxidation of Met[35] retarded the formation of Aβ40 trimer and tetramer,[42] and of Aβ40[43] and Aβ42[44] protofibrils. In addition, there is no consensus with regard to the question of whether oxidation of Met[35] attenuates Aβ toxicity.[37,52] We show here that oxidation of Met[35] dramatically changes the way in which Aβ42 oligomerizes. Paranuclei, which recently have been shown to be characteristic of Aβ42 oligomerization,[33] do not form when Met[35] is oxidized. In fact, [Met(O)[35]]Aβ42 yields an oligomer size distribution characteristic of Aβ40. Replacement of the sulfur atom by a methylene group, as in [Nle[35]]Aβ42, yields a characteristic Aβ42 oligomer size distribution. Substitution of Met[35] by Nle was reported to reduce Aβ fibril-induced neuronal death.[53,54] Studies are now required to determine whether a similar effect is produced by oligomeric [Nle[35]]Aβ42.

Our studies of Aβ oligomerization using [Nle[35]]Aβ42 demonstrate that the sulfur atom is not essential for production of Aβ42 paranuclei. This conclusion is supported by the observation that [Hle[35]]Aβ42 also produces a typical Aβ42-like oligomer distribution. Hle is as nonpolar as Nle but is significantly larger than either Nle or Met (Table 1). Therefore, the polarity, rather than the size, of the residue 35 side-chain appears to be the key factor controlling oligomerization pathway choice. One mechanistic explanation for this phenomenon is that the increased energetic cost of desolvating the oxidized (polar) side chain of Met(O) or Met(O_2) disfavors paranucleus formation. During paranucleus formation, Met likely participates in hydrophobic interactions leading to its exclusion from the solvent-accessible volume—an energetically favorable process for the relatively nonpolar Met side-chain. This hypothesis is supported by comparative examination of the energetics of solvation of dimethyl sulfide (DMS) and dimethyl sulfoxide (DMSO), compounds corresponding to the side chain groups beyond the β-methylene in Met and Met(O), respectively (Table 1). Experimental and computational data demonstrate that the hydration of DMSO is a more favorable process than is the hydration of DMS. The partial molar enthalpy of DMSO at infinite dilution in water is -4.33 kcal/mol.[55] The solvation free energy for DMS is 0.15 kcal/mol[56] and the solvation enthalpy is -2.37 kcal/mol.[56] The increased solubility of DMSO in water can be explained by its tendency to act as a hydrogen bond acceptor.[55] In addition, DMSO has a large dipole moment (3.96 D)[57] compared to the dipole moment of DMS (1.5 D).[57] The dipole moment of dimethyl sulfone ($DMSO_2$) is even larger (4.25 D) than that of DMSO. Oxidation of Met to the sulfoxide or sulfone forms thus produces a substantial dipole moment and makes the oxidized Met[35] a strong hydrogen bond acceptor. This makes the solvation free energy of the residue substantially larger than that of the relatively nonpolar Met residue, a change which would disfavor movement of the side-chain into the apolar environment of the assembled Aβ oligomer. In support of this hypothesis, when Aβ42 and [Met(O)[35]]Aβ42 are mixed in different ratios and cross-linked, the observed oligomer size distributions appear to be simple composites of the distribution of each alloform alone (data not shown). This "titration" of the oligomer size distribution is consistent with a homotypic peptide association process in which reduced and oxidized Aβ molecules do not interact appreciably with each other. Also consistent with this idea is the recent observation that upon oxidation of Met[35], Aβ no longer interacts with phospholipid vesicles.[52]

Table 2. Calculated Side-chain Aqueous Solvation Energy[a]

Residue	G_{cav}	$G_{elec}(\epsilon = 4)$	$G_{elec}(\epsilon = 80)$	ΔG_{elec}
Met	2.85	−0.37	−0.54	0.17
Met(O)	3.05	−3.98	−5.85	1.87
Met(O_2)	3.18	−3.86	−5.68	1.82
Nle	2.85	−0.04	−0.06	0.02
Hle	3.30	−0.05	−0.07	0.02

[a] The cavitation free energy G_{cav}, the peptide solvation free energy $G_{elec}(\epsilon = 4)$, the aqueous solvation free energy $G_{elec}(\epsilon = 80)$, and the "desolvation" energy ΔG_{elec} were calculated as described in the Discussion. Each is expressed in units of kcal/mol.

The relationships between the dipoles and van der Waals volumes corresponding to Met and Met(O_2) demonstrate this effect quantitatively. We assume that the difference in the dipole moment (~3.6 D) between these two side chains is produced by a point dipole placed at the center of the sulfur atom. The distance between the center of the sulfur atom and the solvent exposed surface of the oxygen bound to sulfur is taken to be 3.23 Å.[58] This distance is the minimal radius of the spherical cavity in which the point dipole is placed. The electrostatic contribution to the free energy of the dipole in water can be estimated by the classical theory of Onsager[59]

$$G_{elec} = -\frac{1}{2}\phi_{RF}\mu = -\frac{\mu^2(\epsilon - 1)}{a^3(2\epsilon + 1)}$$

where ϕ_{RF} is the reaction field with which the solvent responds to the dipole, μ is the dipole moment, ϵ is the relative dielectric constant of the solvent (80 for water), and a is the radius of the sphere in which the dipole is placed. For the most polar residues, Met(O) and Met(O_2), the aqueous solvation energy (G_{elec}) is large, thus the sulfoxide and sulfone functions interact favorably with solvent water (Table 2). The influence of the difference in the van der Waals volume can be estimated by evaluating the work necessary to create a cavity with radius a using a solvent accessible surface area (SASA) proportionality relation[60,61]

$$G_{cav} = \gamma A_{SAS}$$

where γ has the dimensions of a surface tension and A_{SAS} is the SASA. The results listed in Table 2 were obtained by choosing 30 cal/(mol Å^2) for γ (for alkanes, the typical value is 20−30 cal/(mol Å^2)[61]). Increasing the volume of Met by oxidation to Met(O) or Met(O_2) leads to a relatively small, unfavorable energetic cost.

In considering the energetic cost of removing an amino acid side-chain from an aqueous solvent ($\epsilon = 80$) and placing it in an internal, hydrophobic cavity ($\epsilon = 4$) in an oligomeric form of a peptide, the "desolvation" energy is the most important

(52) Barnham, K. J.; Ciccotosto, G. D.; Tickler, A. K.; Ali, F. E.; Smith, D. G.; Williamson, N. A.; Lam, Y. H.; Carrington, D.; Tew, D.; Kocak, G.; Volitakis, I.; Separovic, F.; Barrow, C. J.; Wade, J. D.; Masters, C. L.; Cherny, R. A.; Curtain, C. C.; Bush, A. I.; Cappai, R. *J. Biol. Chem.* **2003**.
(53) Varadarajan, S.; Yatin, S.; Kanski, J.; Jahanshahi, F.; Butterfield, D. A. *Brain Res. Bull.* **1999**, *50*, 133−141.
(54) Yatin, S. M.; Varadarajan, S.; Link, C. D.; Butterfield, D. A. *Neurobiol. Aging* **1999**, *20*, 325−330.
(55) Rosenbaum, E. E. *Dimethyl Sulfoxide*; Marcel Dekker: New York, 1971.
(56) Kubo, M. M.; Gallicchio, E.; Levy, R. M. *J. Phys. Chem. B* **1977**, *101*, 10 527−10 534.
(57) Nelson, R. D. J.; Lide, D. R.; Maryott, A. A.; NSRDS-NBS10, 1967.
(58) Strader, M. L.; Feller, S. E. *J. Phys. Chem. A* **2002**, *106*, 1074−1080.
(59) Onsager, L. *J. Am. Chem. Soc.* **1936**, *58*, 1486−1493.
(60) Lee, B.; Richard, F. M. *J. Mol. Biol.* **1971**, *55*, 379−400.
(61) Roux, B. In *Computational Biochemistry and Biophysics*; Becker, O. M., MacKerell, A. D. J., Roux, B., Watanabe, M., Eds.; Marcel Dekker: New York, 2001.

factor. This energetic cost is estimated to be

$$\Delta G_{elec} = G_{elec}(\epsilon = 4) - G_{elec}(\epsilon = 80)$$

A Met(O) or Met(O_2) side-chain partitions preferentially into the aqueous environment, thus its burial in a less polar oligomer core, as would occur during paranucleus formation, is unfavorable. In contradistinction to solvation effects, the relatively large excluded volume of the Hle does not significantly disrupt the formation of small or large oligomers, indicating that steric effects in the packing about residue 35 are of little significance. Our observations are consistent with those of Craik and coworkers,[62] who studied Aβ structural changes due to oxidation of Met[35] in *monomeric* Aβ40 solvated in a water−micelle environment. In the unoxidized peptide (PDB code 1BA4), the side chain of Met[35] lies on the backbone and does not disrupt the local helical structure.[62] In the oxidized peptide (PDB code 1BA6), the side chain of Met(O)[35] is repositioned to make better contact with the aqueous solvent. The exposure of the methionine sulfoxide residue to solvent disrupts the helical structure observed in the WT peptide.[41] Disruption of Aβ helical structure by an Ile[31] → Pro substitution (a region proximal to Met[35]) has been proposed by Butterfield et al. as a mechanism for an observed suppression of oxidative stress and neurotoxicity.[63] Our CD data do not reveal a significant reduction in α-helix content following Met oxidation, suggesting that solvation effects, as opposed to secondary structure changes, are the key determinants of oligomerization state in our experiments.

Previously,[33] we demonstrated that paranucleus formation required an Aβ peptide extending to Ile[41]. The association of paranuclei into higher order assemblies required the addition of Ala[42]. This second assembly step was facilitated by Thr[43] or by replacement of the C-terminal carboxyl by a carboxamide.[48] The data presented here demonstrate that Met[35] is involved directly in formation of Aβ42 paranuclei. It is possible that paranucleus formation involves direct interaction between Met[35] and the Aβ C-terminus, particularly Ile[41]. Experimental evidence exists that the C-terminus of monomeric Aβ42 in aqueous solution does not form a stable structure.[38,64] Thus, an interaction between Met[35] and Ile[41] likely would be intermolecular in nature and occur during Aβ42 oligomerization. Alternatively, both Met[35] and Ile[41] may be critical in controlling the oligomerization of Aβ42 but act independently. Further studies are necessary to evaluate these possibilities.

The observation that the oligomer size distribution and morphology of oxidized Aβ42 are similar to those of Aβ40 suggests that Met[35] oxidation would alter the biological behavior of the resulting Aβ42 oligomers. Oligomeric Aβ40 is less neurotoxic than oligomeric Aβ42.[18,30] If these distinct neurotoxic activities correlate with the quaternary structure of Aβ40 and Aβ42, and oxidation of Met[35] reduces the neuronal injury mediated by Aβ42 oligomers, then oxidizing agents specifically targeting Met[35] within Aβ42 could be valuable therapeutic tools for AD.

Materials and Methods

Peptides and Reagents. Aβ(1−40), [Met(O)[35]]Aβ(1−40), [Met(O_2)[35]]Aβ(1−40), [Nle[35]]Aβ(1−40), [Hle[35]]Aβ(1−40), Aβ(1−42), [Met(O)[35]]Aβ(1−42), [Met(O_2)[35]]Aβ(1−42), [Nle[35]]Aβ(1−42), and [Hle[35]]Aβ(1−42) were synthesized by 9-fluorenylmethoxycarbonyl (FMOC) chemistry, purified by reverse phase HPLC, and characterized by mass spectroscopy and amino acid analysis (AAA), essentially as described.[65] Mass spectrometry was performed using a ThermoFinnigan LCQDeca electrospray ionization/ion trap mass spectrometer linked to a Surveyor HPLC system. Tris(2,2′-bipyridyl)dichlororuthenium(II) (Ru(Bpy)) and ammonium persulfate (APS) were purchased from Sigma (Milwaukee, WI). Polyacrylamide gels, buffers, stains, standards, and equipment for SDS-PAGE were from Invitrogen (Carlsbad, CA).

Isolation of Low Molecular Weight (LMW) Aβ Peptides. LMW Aβ alloforms were isolated by size exclusion chromatography (SEC), as described.[34] Briefly, 170 μL of a 2 mg/mL peptide solution prepared in DMSO was fractionated using a 10/30 Superdex 75 HR column eluted at 0.5 mL/min with 10 mM sodium phosphate, pH 7.4, and the central portion of the included peak was collected during ∼30 s. A 10-μL aliquot of each isolate was taken for AAA to determine the peptide concentration.

Cross-Linking and SDS-PAGE Analysis. Freshly isolated LMW peptides were immediately subjected to PICUP, as described.[34] Briefly, 1 μL of 1 mM Ru(Bpy) and 1 μL of 20 mM APS in 10 mM sodium phosphate, pH 7.4, were added to 18 μL of freshly isolated LMW peptide. The mixture was irradiated with visible light, and the reaction was quenched immediately with 10 μL tricine sample buffer (Invitrogen) containing 5% β-mercaptoethanol (β-ME). The cross-linked oligomer mixtures were analyzed by SDS-PAGE and the intensities quantified by densitometry, as described.[34] The amounts taken for SDS-PAGE analyses were adjusted according to the peptide concentration so that equal amounts of protein were loaded in each lane.

Electron Microscopy. SEC-isolated Aβ peptides were used for these experiments, which were done essentially as described.[47] Briefly, 8 μL of sample were applied to glow-discharged, carbon-coated Formvar grids (Electron Microscopy Sciences, Washington, PA) and incubated for 19 min. The solution was gently absorbed using Whatman grade 1 qualitative filter paper. The grid was incubated with 5 μL of 2.5% glutaraldehyde for 4 min and wicked dry with filter paper. The peptide then was stained with 5 μL of 1% uranyl acetate (Pfaltz & Bauer, Inc., Waterbury, CT) for 3 min. This solution was wicked off, and the grid was air-dried. Samples were examined using a JEOL CX100 electron microscope.

Circular Dichroism Spectroscopy. Immediately following isolation of LMW Aβ, aliquots were placed into a 0.1-cm path length quartz cell (Hellma, Forest Hills, NY). The spectra were recorded on an Aviv Model 62A DS spectropolarimeter (Aviv Associates, Lakewood, NJ) over the wavelength range of 195−260 nm, at 22 °C, as described.[66]

Computational Methods. The electric dipole moments and the excluded volumes for Met, Nle, and Hle were calculated using the version 22 parameter set of the CHARMM program.[67] For Met(O), the parameters proposed by Strander and Feller[58] for dimethyl sulfoxide were used. For the sulfur and the sulfur oxygens in Met(O_2), the HF/6-31g* calculated partial charges for dimethyl sulfone[68] were used.

Acknowledgment. We thank Drs. Erica Fradinger, Noel Lazo, and Samir Maji for valuable discussions and criticism. This work

(62) Coles, M.; Bicknell, W.; Watson, A. A.; Fairlie, D. P.; Craik, D. J. *Biochemistry* **1998**, *37*, 11 064−11 077.
(63) Kanski, J.; Aksenova, M.; Schoneich, C.; Butterfield, D. A. *Free Rad. Biol. Med.* **2002**, *32*, 1205−1211.
(64) Zagorski, M. G.; Shao, H.; Ma, K.; Yang, J.; Li, H.; Zeng, H.; Zhang, Y.; Papolla, M. *Neurobiol. Aging* **2000**, *21*, S10−S11 (Abstract 48).
(65) Lomakin, A.; Chung, D. S.; Benedek, G. B.; Kirschner, D. A.; Teplow, D. B. *Proc. Natl. Acad. Sci. U.S.A.* **1996**, *93*, 1125−1129.
(66) Kirkitadze, M. D.; Condron, M. M.; Teplow, D. B. *J. Mol. Biol.* **2001**, *312*, 1103−1119.
(67) Mackerell, A. D.; Bashford, D.; Bellott, M.; Dunbrack, R. L.; Evanseck, J. D.; Field, M. J.; Fischer, S.; Gao, J.; Guo, H.; Ha, S.; Josephmccarthy, D.; Kuchnir, L.; Kuczera, K.; Lau, F. T. K.; Mattos, C.; Michnick, S.; Ngo, T.; Nguyen, D. T.; Prodhom, B.; Reiher, W. E.; Roux, B.; Schlenkrich, M.; Smith, J. C.; Stote, R.; Straub, J.; et al. *J. Phys. Chem. B* **1998**, *102*, 3586−3616.
(68) Johnson, R. D. I.; Richter, U.; Manichaikul, A.; Schneider, B.; Release 7 ed.; National Institute of Standards and Technology, 2002.

was supported by Grants NS44147, AG18921, and NS38328 from the National Institutes of Health (D.B.T.), by the Foundation for Neurologic Diseases (D.B.T.), and by Grant No. 1042312909A1 from The Massachusetts Alzheimer's Disease Research Center (G.B.).

Supporting Information Available: CD spectra for all the Aβ alloforms used in this work. This material is available free of charge via the Internet at http://pubs.acs.org

JA0349296